Chapter 12
Modern Experiments on Atom-Surface Casimir Physics

Maarten DeKieviet, Ulrich D. Jentschura and Grzegorz Łach

Abstract In this chapter we review past and current experimental approaches to measuring the long-range interaction between atoms and surfaces, the so-called Casimir-Polder force. These experiments demonstrate the importance of going beyond the perfect conductor approximation and stipulate the relevance of the Dzyaloshinskii-Lifshitz-Pitaevskii theory. We discuss recent generalizations of that theory, that include higher multipole polarizabilities, and present a list of additional effects, that may become important in future Casimir-Polder experiments. Among the latter, we see great potential for spectroscopic techniques, atom interferometry, and the manipulation of ultra-cold quantum matter (e.g. BEC) near surfaces. We address approaches based on quantum reflection and discuss the atomic beam spin-echo experiment as a particular example. Finally, some of the advantages of Casimir-Polder techniques in comparison to Casimir force measurements between macroscopic bodies are presented.

12.1 Introduction

In this chapter we will be dealing with experimental aspects of the Casimir-Polder force. (See Chap. 11 by Intravaia et al. in this volume for additional discussions about the theoretical aspects of the Casimir-Polder force.) Although no strict criterion can be implied to distinguish between the Casimir and the Casimir-Polder

M. DeKieviet (✉) · G. Łach
Physikalisches Institut der Universität Heidelberg, Philosophenweg 12,
69120, Heidelberg, Germany
e-mail: maarten.dekieviet@physi.uni-heidelberg.de

U. D. Jentschura
Department of Physics, Missouri University of Science and Technology,
Rolla, MO 65409-0640, USA

effect, it is common use to describe the interaction between two macroscopic, polarizable (neutral and nonmagnetic) bodies due to the exchange of virtual photons as Casimir interactions. In contrast, Casimir-Polder effects should involve at least one microscopic, polarizable body, typically an atom or molecule. Although the transition from Casimir to Casimir-Polder physics is a continuous one,[1] the distinction goes back to the seminal 1948 paper by Casimir and Polder [1]. Herein, the authors discuss the influence of retardation on the London-van der Waals forces. In particular, they derive the long-distance behavior of the quantum electrodynamic interaction between an atom and a perfectly conducting surface and that between two atoms. The works by Casimir and Casimir and Polder address the fact that the mutually induced polarization between two neighboring objects may be delayed as a consequence of the finiteness of the velocity of light. The Casimir and the Casimir-Polder forces could thus semiclassically be termed long-range retarded dispersion van der Waals forces. Indisputably the two 1948 papers by Casimir and Casimir and Polder mark the beginning of a whole new branch of research addressing fundamental questions about quantum field theory in general and the structure of the vacuum in particular. The concepts developed in 1948 are now being used in order to describe a rich field of physics, and have been supplemented by a variety of methods to address also practically important areas of applications. Especially with the rise of nanotechnology, there is a growing need for a quantitative understanding of this interaction and experimental tests are indispensable.

12.2 The History of Casimir-Polder Experiments

Before we turn to modern aspects of Casimir-Polder physics it is useful to review some of the developments that led us here. The correct explanation for the non-retarded dispersive van der Waals interaction between two neutral, but polarizable bodies was possible only after quantum mechanics was properly established. Using a perturbative approach, London showed in 1930 [2] for the first time that the above mentioned interaction energy is approximately given by

$$\mathcal{V}_{London}(z) \approx -\frac{3\hbar\omega_0 \alpha_1^A \alpha_1^B}{2^6 \pi^2 \varepsilon_0^2 z^6} \tag{12.1}$$

where α_1^A and α_1^B are the static dipole polarizabilities of atoms A and B, respectively. ω_0 is the dominant electronic transition frequency and z is the distance between the objects. Experiments on colloidal suspensions in the 1940s by Verwey and Overbeek [3] showed that London's interaction was not correct for large distances. Motivated by this disagreement, Casimir and Polder were the first in

---

[1] It is in fact a useful and instructive exercise to derive the latter from the former by simple dilution.

1948 to consider retardation effects on the van der Waals forces. They showed that in the retarded regime the van der Waals interaction potential between two identical atoms is given by

$$\mathscr{V}_{retard}(z) = -\frac{23\hbar c \alpha_1^A \alpha_1^B}{2^6 \pi^3 \varepsilon_0^2 z^7}. \tag{12.2}$$

The reason is that, at larger separations, the time needed to exchange information on the momentary dipolar states between the two objects may become comparable to or larger than the typical oscillation period of the fluctuating dipole. The length scale at which this happens can be expressed in terms of a reduced wavelength $\lambdabar$ of the lowest allowed atomic transition that relates to the transition frequency ω_0 (or wavelength λ) and the speed of light c

$$z \geq \frac{c}{\omega_0} = \frac{\lambda}{2\pi} = \lambdabar. \tag{12.3}$$

The onset of retardation is thus a property of the system. In their paper, Casimir and Polder also showed that the retarded van der Waals interaction potential between an atom and a perfectly conducting wall falls at large distances as $1/z^4$, in contrast to the result obtained in the short-distance regime (non-retarded regime), where it is proportional to $1/z^3$. They derived a complete interaction potential valid also for intermediate distances. By the use of the dynamic polarizability of the atom $\alpha(i\omega)$ the Casimir and Polder result can be rewritten as

$$\mathscr{V}^{\infty}(z) = -\frac{\hbar}{(4\pi)^2 \varepsilon_0 z^3} \int_0^{\infty} d\omega \alpha_1(i\omega) \left[1 + 2\frac{\omega z}{c} + 2\left(\frac{\omega z}{c}\right)^2 \right] e^{-2\omega z/c}. \tag{12.4}$$

Its short-range limit, equivalent to the nonrelativistic approximation ($c \to \infty$) reproduces the van der Waals result for the atom-surface interaction energy

$$\mathscr{V}^{\infty}(z) \overset{z \to 0}{=} -\frac{\hbar}{(4\pi)^2 \varepsilon_0 z^3} \int_0^{\infty} d\omega \alpha_1(i\omega). \tag{12.5}$$

The long-distance limit for the perfect conductor case is especially important and has become the signature for the Casimir-Polder force

$$\mathscr{V}^{\infty}(z) \overset{z \to \infty}{=} -\frac{3\hbar c \alpha(0)}{2^5 \pi^2 \varepsilon_0 z^4}. \tag{12.6}$$

In the 1960s, Lifshitz and collaborators developed a general theory of van der Waals forces [4] and extended the result of Casimir and Polder to arbitrary solids. (See also the Chap. 2 by Pitaevskii in this volume for additional discussions about the Lifshitz theory.) Their continuum theory is valid for both dielectrics and semiconductors, and for conductors, as long as their electromagnetic properties can be described by a local $\varepsilon(\omega)$. The result for a perfect conductor is recovered by

taking the limit of infinite permittivity: $\varepsilon(\omega) \to \infty$. Lifshitz [4] computed the interaction energy between an atom and a realistic material, described by its frequency dependent permittivity evaluated for imaginary frequencies $\varepsilon(i\omega)$. His result gives the dominant contribution for large atom-surface distances, and reads

$$\mathscr{V}(z) = -\frac{2\hbar}{(4\pi)^2 \varepsilon_0 c^3} \int\limits_0^\infty d\omega \omega^3 \alpha_1(i\omega) \int\limits_1^\infty d\xi e^{-2\xi\omega z/c} H(\xi, \varepsilon(i\omega)), \qquad (12.7)$$

where the $H(\xi, \varepsilon)$ function is defined as

$$H(\xi, \varepsilon) = (1 - 2\xi^2) \frac{\sqrt{\xi^2 + \varepsilon - 1} - \varepsilon\xi}{\sqrt{\xi^2 + \varepsilon - 1} + \varepsilon\xi} + \frac{\sqrt{\xi^2 + \varepsilon - 1} - \xi}{\sqrt{\xi^2 + \varepsilon - 1} + \xi}. \qquad (12.8)$$

The Lifshitz formula (12.7) reproduces the Casimir and Polder result (12.4) for perfect conductors. Both in the short- and the long-range limits, the Lifshitz formula simplifies considerably. For $z \to 0$ the interaction potential behaves as

$$\mathscr{V}(z) \overset{z \to 0}{\sim} -\frac{\hbar}{(4\pi)^2 \varepsilon_0 z^3} \int\limits_0^\infty d\omega \alpha_1(i\omega) \frac{\varepsilon(i\omega) - 1}{\varepsilon(i\omega) + 1} \equiv -\frac{C_3}{z^3}. \qquad (12.9)$$

In the long-distance limit the interaction potential for a generic $\varepsilon(\omega)$ is

$$\mathscr{V}(z) \overset{z \to \infty}{\sim} -\frac{3\hbar c \alpha_1(0)}{2(4\pi)^2 \varepsilon_0 z^4} \frac{\varepsilon(0) - 1}{\varepsilon(0) + 1} \equiv -\frac{C_4}{z^4}. \qquad (12.10)$$

Under some special conditions the Casimir and Polder force can also be inferred (both theoretically and experimentally) from the interaction energy of two macroscopic bodies, if we consider one of the media sufficiently dilute [5]. These conditions were fulfilled in the experiments by Sabisky and Anderson [6]. In this sense this 1972 experiment can be viewed as the first experimental verification of the Casimir-Polder force. In their beautiful cryogenic experiments Subisky and Anderson measured the thickness of helium films adsorbed on cleaved SrF_2 surfaces in thermal equilibrium at 1.4 K as a function of hyperpressure. The authors get exceptionally good agreement between the film thickness measured and the one calculated using the Lifshitz formula. The agreement is even more remarkable since the method strongly depends on the assumption that the non-additivity of the van der Waals forces does not play a major role. In this case that assumption works so well because of the extraordinary weakness of the interaction between helium atoms. The authors note that the best results were obtained on atomically flat regions of the substrate and that the influence of surface roughness in these experiments was certainly significant.

Only two years later Shih and Parsegian [7] published an atomic beam deflection experiment to measure van der Waals forces between heavy alkali atoms and gold surfaces. With these precision measurements the authors were able for the first time to pin down the distance dependency of the van der Waals force in

Fig. 12.1   The Cs beam profile, normalized to the full beam intensity, measured as a function of the deflection distance S, into the geometric shadow of the gold surface. The derived interaction potential is consistent with the van der Waals form $1/z^3$ and has a strength which is best described within the macroscopic continuum theory of Lifshitz. (Reproduced with permission from [7].)

THEORETICAL PROFILE
BASED ON THE
LIFSHITZ POTENTIAL

I/I_o

Cs ON GOLD

0.04   0.08   0.12 cm
S
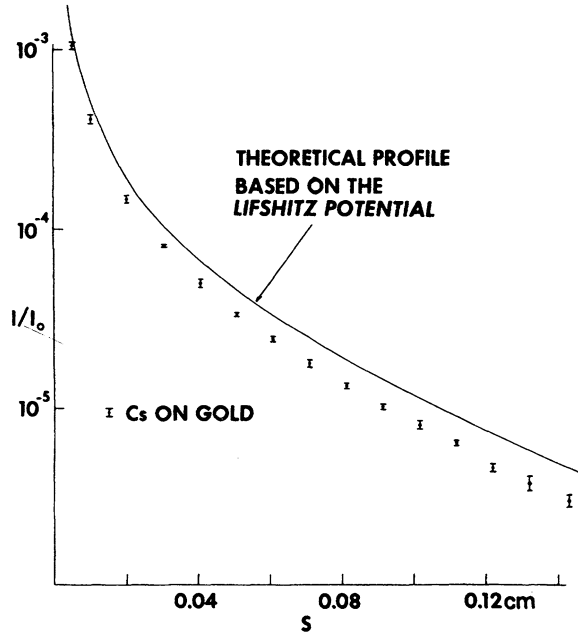
the non-retarded regime to be proportional to $1/z^3$. The authors include very accurate calculations of the interaction potential performed using the Lifshitz formula. They used *ab-initio* computed (on the Hartree-Fock level) atomic po-larizabilities and included the finite conductivity of the gold substrate. The resulting strength coefficient C_3 of the van der Waals interaction is not a constant but varies with separation (the retardation effect). Unfortunately, the measure-ments (see Fig. 12.1) were not precise enough in the region of interest to reveal these retardation effects as a deviation from the $1/z^3$ behavior. It is worth noting that although these calculations were the best available at the time the theoretical values they predict are systematically 60% larger than the values for the interac-tion observed in experiments. The authors suggest surface roughness and con-tamination as possible sources for the discrepancy between calculation and experiment. Still, this seminal paper is the first definite confirmation of the validity of the Dzyaloshinskii-Lifshitz-Pitaevskii [8] formalism for the interaction between an atom and a surface, and establishes QED vacuum fluctuations as the common basis for van der Waals and Casimir-Polder forces.

It took almost two more decades before a deviation from the $1/z^3$ behavior for the van der Waals potential was experimentally resolved. In Ed Hinds's group [9] a beam of ground state sodium atoms was passed through a micron-sized cavity. This geometry does not exactly correspond to the Casimir-Polder atom single plate arrangement, but instead the atoms travel slowly through a cavity made of plates that include a small angle (V-shape). The cavity width can be varied by moving the source vertically. As a function of plate separation the transmission loss due to the

long-range interaction with the cavity walls was measured and compared to Monte-Carlo simulations. At large plate distances the purely geometric losses dominate, but below a critical width Casimir-Polder losses become significant.[2] Hinds et al. could clearly show a modification of the ground state Lamb shift for the sodium atoms within the cavity, scaling as $1/z^4$. Furthermore, the numerical coefficient of the $1/z^4$ interaction was found to be in agreement with theory. Unfortunately the data do not show a smooth transition to the expected van der Waals behavior at short distances. The experiment relies heavily on the fact that any atoms not traveling through the center of the cavity are accelerated towards one of the two plates, stick there and are thus removed from the beam. This accumulation and its influence on the spectral properties of the plates were not taken into account.

With the advent of methods for laser cooling and manipulating atoms it became possible to use light in order to control ultracold atom-wall collisions. Aspect et al. [10] were the first to use laser cooled and trapped atoms to investigate the Casimir-Polder potential. ^{87}Rb atoms, caught at a temperature of 10 μK, were released from a magneto-optical trap into the gravitational potential. After 15 mm of free fall, the ultracold beam of ^{87}Rb atoms impinged at normal incidence on an atomic mirror. This mirror consists of a prism that is irradiated from the back by laser light. This laser light forms an evanescent wave extending along the face of the dielectric, and as it is slightly detuned from the atomic resonance frequency of the ^{87}Rb atoms it can provide a controlled repulsive potential for the atoms. Within this light potential the equilibrium between a repulsive light force and the attractive surface interaction is used to establish a potential barrier that can be well controlled by changing the light field. The reflectivity for incident atoms is measured as a function of barrier height. Landragin's data seem to favor the inclusion of retardation effects in the atom-wall interaction potential.

In 2001 Shimizu succeeded in reflecting very slow metastable neon atoms specularly from a solid surface[3] [11]. Shimizu prepared an ultracold beam of neon atoms by trapping the metastables in a magneto-optical trap and then releasing them into the gravitational potential. After tens of centimeters of free fall, the metastables impinged under grazing incidence on the substrate. By varying the angle of incidence he could change the normal incident velocity of the metastable neon atoms between 0 and 35 mm/s. New in his approach was that the quantum reflectivity, that is the reflection from the attractive part of the interaction potential only, depends heavily on the perpendicular impinging energy of the particle. Plotting the reflectivity of metastable neon atoms versus the normal incident velocity of the beam the author was able to uniquely identify that the attractive

---

[2] It is not entirely clear how much of the nontrivial geometrical effects were taken into account in the data analysis.

[3] In early experiments of quantum deflecting H atoms, liquid helium was used as a target. Collectiveness of He atoms within the fluid was ignored, giving information only on the H–He interatomic potential. It is not quite clear how many of the exotic properties of this superfluid have an effect on the interaction potential with this macroscopic quantum object.

interaction was of the Casimir-Polder sort, that is having a $1/z^4$ dependency. A simple combined van der Waals Casimir-Polder potential was used to fit the data, but the measurements were not accurate enough to allow for a quantitative comparison with theory. The surfaces Shimizu used were rough on a scale much larger than the de Broglie wavelength of the atoms. This and the fact that the Ne atoms were in a metastable state guarantees that none of the atoms is specularly reflected from the repulsive core potential at short distances.[4]

In 2003 our group published the first experimental observation of quantum reflection of ground state atoms from a solid surface [12]. Using the extreme sensitivity of the earlier developed atomic beam spin echo method [13] we monitored ultracold collisions of ^{3}He atoms from the rough surface of a quartz single crystal. The roughness of the substrate guaranteed that the reflection could only originate from the attractive part of the potential. The quantum reflectivity data confirmed the theory by Friedrich et al. [14] on the asymptotic behavior of the quantum reflection probability at incident energies far from the threshold $E_i \rightarrow 0$.[5] The data confirm this high energy asymptotic behavior which is determined by the van der Waals interaction and show a gradual transition towards the retarded regime starting as early as 30 Å above the surface. From the data the gas-solid interaction potential is deduced quantitatively covering both regions. Using a simple approximation for the inhomogeneous attractive branch of the helium-quartz interaction potential

$$\mathcal{V}(z) = -\frac{C_4}{z^3(z+\hat{\lambda})} \tag{12.11}$$

we find excellent quantitative agreement with the quantum reflection experimental data for the potential coefficient $C_4 = 23.6$ eV Å^3 and the reduced atomic transition wavelength $\hat{\lambda} = 93$Å. The experiment establishes quantitative evidence for the $1/z^4$ Casimir-Polder attraction and the transition towards the $1/z^3$ van der Waals regime. Surface roughness was taken into account explicitly, based on an ex-situ atomic force microscopic measurement. It is worthwhile stressing that both the atom and the substrate are in their ground state and no lasers are involved. It thus represents the situation of a single atom interacting with a well defined, extended, dielectric body through the virtual photons of the quantum fluctuating vacuum exclusively quite accurately.

The experimental data were also investigated with respect to the inhomogeneity of the potential model used in (12.11). The analysis shows that neither of the two homogeneous parts, the van der Waals and the Casimir-Polder branches, can describe the data without the inclusion of the other. Even though at the distances explored in this experiment the energies are dominated by the van der Waals interaction, there is a definite need to include the Casimir-Polder term explicitly.

---

[4] Mind that metastables may exchange real photons with the substrate.

[5] For a review on WKB waves far from the semiclassical limit see [15] and references therein.
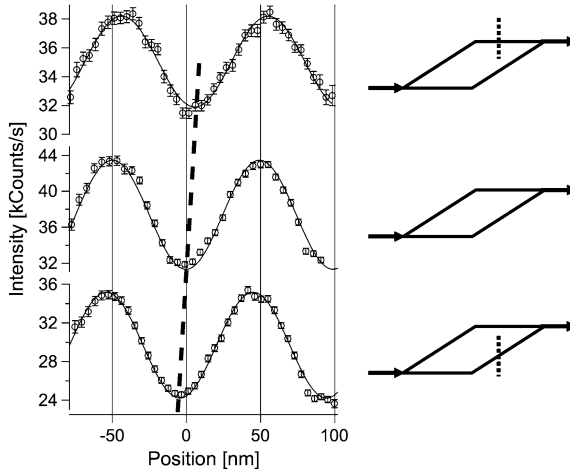
Fig. 12.2 Interference pattern observed for sodium atoms passing the atom interferometer without a grating (*middle*), or when the grating is inserted into path α (*upper*) or path β (*lower*). The dashed line illustrates the measured phase shift of 0.3 rad. From the measured induced phase shift as a function of atomic velocity, the authors obtain a van der Waals coefficient $C_3 = 3$ meV nm^3. (Reproduced with permission from [16].)

This stipulates that the onset of retardation is not only smooth, but extends to well within the van der Waals regime.

Around the same period, Perreault and Cronin [16] used an atom interferometer, in which a well collimated beam of sodium atoms illuminates a silicon nitride grating with a period of 100 nm. During passage through the grating slots atoms acquire a phase shift due to the van der Waals interaction with the grating walls. As a result the relative intensities of the matter-wave diffraction peaks deviate from those expected for a purely absorbing grating. A complex transmission function was developed to explain the observed diffraction envelopes. By fitting a modified Fresnel optical theory to the experimental data the authors obtain a van der Waals coefficient $C_3 = 2.7 \pm 0.8$ meV nm^3 for the interaction between atomic sodium and a silicon nitride surface. A few years later, the experiment was refined by going to a 50 nm wide cavity. The magnitude of the measured phase shift (see Fig. 12.2) caused by atom-surface interaction is in agreement with that predicted by quantum electrodynamics for a non-retarded van der Waals interaction.

Steady progress in laser cooling and quantum optics and the application of evaporative cooling at the turn of the century led to the first successful creation of a macroscopic quantum system. Nowadays Bose-Einstein condensates are produced routinely in dozens of labs all over the world. Their behavior and stability in the vicinity of a solid wall has been investigated for both fundamental and technical reasons. The first such experiment focusing on the Casimir-Polder interaction was performed in the group of Ketterle [17] using a Bose-Einstein condensate of ^{23}Na atoms. Since the BEC is much colder than the thermal ensemble in a MOT

(magnetic-optical trap), like the one Shimizu used, the authors observed quantum reflectivity for incident angles up to normal. Another major difference is that the silicon substrate used in this experiment is approached while the atoms are still trapped in a weak gravito-magnetic trap. The measured reflection probability as a function of incident normal velocity was compared with a numerical simulation done for sodium atoms interacting with a conducting wall. The comparison shows qualitative agreement. Even though the authors simulate the interaction between the sodium atoms and the semiconductive surface through a C_4 coefficient which corresponds to a conducting surface, the calculated reflection probability is still systematically higher than the measured data points. The experiment confirms the $1/z^4$ behavior but the range of velocities the authors could explore is not large enough to investigate the region closer to the surface where the potential has $1/z^3$ dependence. The authors refer to earlier work by Cornell et al. [18] (see also Chap. 11 by Intravaia et al. in this volume for additional discussions) and Vuletic [19], who discuss serious problems that condensate-based experiments near surfaces may experience due to the pollution of even only a small number of atoms at the surface. Spurious electric and magnetic fields caused by the adsorbates may lead to large local anomalies in the interaction potential and may severely limit sensitive Casimir-Polder force measurements.[6] A few years later, a refined version of the experiment was published and interpreted as a measurement of the temperature dependence of the Casimir-Polder force [20]. In the analysis, however, the temperature dependence of the coverage and the IR properties of the adsorbates were not included. In a recent experiment by Zimmermann et al. [21], which is comparable to the experiment in [10], an unresolved inconsistency in the quantitative comparison between Casimir-Polder theory and experiment is still present.

It is fair to say that in present day Casimir-Polder physics the quantitative comparison between experiments and theory is limited by the lack of detailed knowledge of the exact experimental parameters like surface roughness and cleanliness, identity of the adsorbates and their influence on the overall atom-surface interaction potential. Consequently, modern experiments on atom-surface Casimir physics should not only aim for higher precision, but simultaneously for a better characterization and control of these experimental conditions.

Before discussing the different experimental approaches in this context, it may be useful to identify the physics that could possibly be revealed in future Casimir-Polder studies. In the following section we summarize some of the current theoretical issues.

---

[6] In [17] Ketterle makes the following observation: "Surfaces are traditionally considered enemies of cold atoms: Laser cooling and atom optics have developed thanks to magnetic and optical traps that confine atoms with non-material walls in ultrahigh vacuum environments designed to prevent contact with the surfaces. Paradoxically, it turns out that in the extreme quantum limit of nano Kelvin matter waves, a surface at room temperature might become a useful device to manipulate atoms."

12.3 The Atom-Surface Interaction

12.3.1 Practical Application of the Lifshitz Formula

The properties of the solid enter the formula (12.7) in the form of its frequency
dependent permittivity. Although it has been demonstrated that ε can in some cases
be computed *ab-initio* [22], the accuracy and reliability of the obtained results are
uncertain at present. Possible difficulties include the contribution of vibrational
excitations within the solid to the atom-surface interaction energy [23]. This term
can be relatively large, like in the case of glass or $\alpha-$quartz (10%) and has so far
been neglected in the full *ab-initio* approach.

Some of the solids for which the contemporary experiments are performed are
transition metals, for which both the relativistic effects and the fact that metals are
open shell systems make accurate theoretical predictions extremely difficult.
Another drawback of the presently available theoretical results for solids is the
neglect of temperature effects. As a result the theoretically computed permittivity
as a function of frequency typically exhibits more structure than the ones derived
from experimental optical data. This makes the use of published optical data a
useful alternative to theoretical computation of the dielectric properties of solids
(e.g. [24] and references therein). The procedure, however, is complicated by the
fact that experimental data for the complex permittivity exist only for real fre-
quencies and its values along the imaginary axis have to be reconstructed using the
Kramers-Kroenig relation:

$$\varepsilon(i\omega) = 1 + \frac{2}{\pi} \int\limits_{0}^{\infty} d\xi \frac{\xi \operatorname{Im}\varepsilon(\xi)}{\omega^2 + \xi^2}. \tag{12.12}$$

Apart from the frequency dependent permittivity of the solid the computation of
the atom-surface interaction energy requires the dynamic dipole (or multipole)
polarizability of the atom as an input. In the past a single resonance model for the
dynamic polarizability was used:

$$\alpha_1(i\omega) = \frac{\alpha_1(0)}{1 + \omega^2/\omega_1^2}, \tag{12.13}$$

where ω_1 is the lowest allowed transition frequency. This simplification may lead
to an error in the short range interaction energy as large as 40% (for the case of He)
when compared to results that use more accurate polarizabilities. Slight
improvement is obtained by using a few-resonance approximation, in which a few
lowest lying excited states are included in the spectral expansion:

$$\alpha_1(i\omega) = \sum_i \frac{f_{i0}^{(1)}}{\omega_i^2 + \omega^2}, \tag{12.14}$$

where ω_i denote the allowed transition frequencies, and $f_{i0}^{(1)}$ (see for example [23])
are the corresponding oscillator strengths. Even when all discrete transition frequencies are included, this approximate approach still leads to a 20% error (for ground state He) as it neglects the significant contribution coming from excitations to the continuous spectrum. We therefore recommend using *ab-initio* computed dynamic atomic polarizabilities whenever possible. Dynamic polarizabilities of the noble gas, alkali and alkaline atoms evaluated for imaginary frequencies have recently been published [25].

12.3.2 Limitations of the Lifshitz Theory

The Lifshitz formula describes the interaction of an arbitrary atom with any surface and is a good starting point for the comparison between atom-surface theory and experiment. It should be realized, however, that it suffers from a number of drawbacks that may become important in future Casimir-Polder experiments. As pointed out earlier, formula (12.7) becomes invalid for atom-surface distances comparable to the charge radius of the atom (of the order of Å), due to exchange effects. At slightly larger distances, of the order of a few Å (for ground state atoms, but as large as a few nm for metastable helium atoms), the Lifshitz approach, being based on second order perturbation theory, breaks down due to higher order effects. At even larger distances (a few nm for He) its validity is reduced further, when quadrupole and higher multipole polarizabilities of the atom are to be included. These effects can be theoretically computed and are considered in the next sections. These, and other corrections to the Lifshitz formula, that cannot easily be assigned a definite length scale will be considered in the following sections. Their list includes:

- Corrections from higher orders of perturbation theory
- Contributions from higher multipole polarizabilities of the atom
- Temperature effects
- Relativistic and radiative corrections
- Effects of magnetic susceptibilities of both the atom and the solid
- Corrections from the nonplanar geometry and imperfections of the surface

From the experimental point of view some of these effects are already in reach with current methods. Others, like the relativistic and radiative corrections, or the effects of nonlocal response of the surface, may only become visible in future generations of experiments.

12.3.3 Higher Orders of Perturbation Theory

The applicability of the Lifshitz formula is limited to distances z larger than $\sqrt[3]{\alpha_1(0)/(4\pi\varepsilon_0)}$, at which higher orders of perturbation theory become important.

The next nonzero contribution to the atom-surface interaction energy comes from the fourth order in atom-field coupling, i.e. second order in atomic dipole polarizability. This has been calculated by Marvin and Toigo [26] and reads

$$\mathscr{V}_{1,1}(z) = -\frac{\hbar}{2^9 \pi^2 \varepsilon_0 z^6} \int_0^\infty d\omega \alpha_1^2(i\omega) \left[\frac{\varepsilon(i\omega) - 1}{\varepsilon(i\omega) + 1}\right]^2 e^{-2\omega z/c} P_{1,1}(\omega z/c), \quad (12.15)$$

where the polynomial $P_{1,1}(x)$ is defined as

$$P_{1,1}(x) = 3 + 12x + 16x^2 + 8x^3 + 4x^2. \quad (12.16)$$

The $\{1, 1\}$ index indicates that (12.15) depends on the square of the dipole polarizability of the atom. It is only the first term of the series of corrections and the ones depending on products of multipole polarizabilities followed by $\mathscr{V}_{1,2}$, $\mathscr{V}_{1,3}$, $\mathscr{V}_{2,2}$, $\mathscr{V}_{1,1,1}$, etc., all of which are at present not calculated.

It is worth noting that together with the above result the same authors present an incorrect formula for the first order term, given here in (12.7). Their leading order result [26] including retardation is in disagreement with [4, 23, 27]. Its short-range, nonrelativistic limit is, however, in agreement with other works. The short-range limit of (12.15) is

$$\mathscr{V}_{1,1}(z) = -\frac{\hbar}{2^9 \pi^2 \varepsilon_0 z^6} \int_0^\infty d\omega \alpha_1^2(i\omega) \left[\frac{\varepsilon(i\omega) - 1}{\varepsilon(i\omega) + 1}\right]^2 \quad (12.17)$$

and is consistent with the nonrelativistic result of McLachlan [28].

12.3.4 Effect of Multipole Polarizabilities

Another group of effects limiting the use of (12.7) are those resulting from the higher multipole polarizabilities of the atom, like quadrupole and octupole ones. The corrections from quadrupole polarizability of the atom become important when z is comparable to $\sqrt{\alpha_2(0)/\alpha_1(0)}$, where α_1 and α_2 denote the dipole and quadrupole polarizabilities of the atom.

The effects of the quadrupolar polarizability of the atom on interaction potential $\mathscr{V}_2(R)$ were first calculated in the nonrelativistic case by Zaremba and Hutson [29]. In general the second order interaction energy can be written as a multipole expansion

$$\mathscr{V}(z) = \mathscr{V}_1(z) + \mathscr{V}_2(z) + \mathscr{V}_3(z) + \cdots \quad (12.18)$$

where each of the $\mathscr{V}_n(z)$ terms comes from the 2^n-pole atomic polarizability coupled to the fluctuating electromagnetic field. The first term $\mathscr{V}_1(z)$ is the

previously considered Lifshitz contribution, while the next ones constitute corrections, which in the limit of small distances behave as C_{2n+1}/z^{2n+1}.

For short distances, higher terms in the multipole expansion used to derive (12.7) become important. The generalization of the derivation of the Lifshitz formula to include higher multipoles has been presented in [23], and gives contributions to the interaction energy from an arbitrary 2^n-pole polarizability of the atom:

$$\mathscr{V}_n(z) = -\frac{\hbar}{8\pi^2\varepsilon_0 c^{2n+1}} \int\limits_0^\infty \mathrm{d}\omega\, \omega^{2n+1}\alpha_n(\mathrm{i}\omega) \int\limits_1^\infty \mathrm{d}\xi \mathrm{e}^{-2\xi\omega z/c} \mathrm{P}_n(\xi)\mathrm{H}(\xi, \varepsilon(\mathrm{i}\omega)),$$
(12.19)

where $\alpha_n(\omega)$ is the 2^n-pole polarizability and $\mathrm{P}_n(\xi)$ are polynomials which for $n = 1, 2, 3, 4$ (dipole, quadrupole, octupole and hexadecupole components) explicitly read

$$\mathrm{P}_1(\xi) = 1,$$
(12.20a)

$$\mathrm{P}_2(\xi) = \frac{1}{6}(2\xi^2 - 1),$$
(12.20b)

$$\mathrm{P}_3(\xi) = \frac{1}{90}(4\xi^4 - 4\xi^2 + 1),$$
(12.20c)

$$\mathrm{P}_4(\xi) = \frac{1}{90}(8\xi^6 - 12\xi^4 + 6\xi^2 - 1).$$
(12.20d)

In the limit of small distances or, equivalently, in the nonrelativistic limit $(c \to \infty)$ (12.19) leads to a surprisingly simple result:

$$\mathscr{V}_n(z) \stackrel{z\to 0}{=} -\frac{\hbar}{(4\pi)^2\varepsilon_0 z^{2n+1}} \int\limits_0^\infty \mathrm{d}\omega\alpha_n(\mathrm{i}\omega)\frac{\varepsilon(\mathrm{i}\omega) - 1}{\varepsilon(\mathrm{i}\omega) + 1}.$$
(12.21)

The $n = 2$ case reproduces the short-range asymptotic result of Zaremba and Hutson [29]. The derivation of the long-distance limit of the multipole contributions lead to

$$\mathscr{V}_n(z) \stackrel{z\to\infty}{=} -\frac{\hbar c\alpha_n(0)}{(4\pi)^2\varepsilon_0 z^{2n+2}} D_n \frac{\varepsilon(0) - 1}{\varepsilon(0) + 1},$$
(12.22)

where the D_n constants are: $D_1 = 3/8$, $D_2 = 25/12$, $D_3 = 301/120$, $D_4 = 1593/560$.

The quadrupole and octupole dynamic atomic polarizabilities of helium atoms (in the ground and metastable states) together with accurate (at 10^{-8}) and simple global fits have been published [30]. Simulations based on potentials computed using these multipole polarizabilities have shown that, in the quantum reflection experiments of the type reported in [12], the quadrupolar contribution could be seen at the few percent level.

12.3.5 Effects of Non-zero Temperature

Modification of the atom-surface interaction energy due to non-zero temperature has two distinct origins. The permittivity of the solid, entering the formulae (12.7)–(12.19), is itself temperature dependent. More importantly there is also an explicit temperature dependence resulting from thermal fluctuations of the electromagnetic field, calculated first by Dzyaloshinskii et al. [8]. The complete formula in a form closely resembling (12.7) reads [31, 32]

$$\mathscr{V}_1(z;T) = \frac{\hbar k_B T}{4\pi\varepsilon_0} \sum_{i=0}^{\infty} (1 - \frac{1}{2}\delta_{0i})\alpha_1(i\omega_i) \int\limits_1^{\infty} d\xi e^{-2\xi\omega_i/c} H(\xi, \varepsilon(i\omega_i)), \qquad (12.23)$$

where k_B is the Boltzmann constant, $\omega_i = 2\pi i k_B T z/\hbar$ are the Matsubara frequencies and $\delta_{0i} = 1$ for $i = 0$, and is equal to 0 otherwise. The above result relies on the assumption that the temperature is small enough to neglect thermal excitations of the atom. This assumption is true as long as $\hbar\omega_1 \gg k_B T$, which is fulfilled for most ground state atoms at any reasonable temperature (i.e. below the melting point of the experimentally considered solids), but does not have to be true for experiments with metastable excited states.

Just as for the $T = 0$ case, in the short-range limit formula (12.23) can be approximated by

$$\mathscr{V}_1(z;T) \stackrel{z\to 0}{=} -\frac{C_3(T)}{z^3}, \qquad (12.24)$$

where

$$C_3(T) = \frac{\hbar k_B T}{16\pi\varepsilon_0} \left[\alpha(0)\frac{\varepsilon(0)-1}{\varepsilon(0)+1} + 2\sum_{i=1}^{\infty} \alpha(i\omega_i)\frac{\varepsilon(i\omega_i)-1}{\varepsilon(i\omega_i)+1} \right]. \qquad (12.25)$$

In the low temperature limit the above result approaches the $T = 0$ one (12.9). It has already been discovered by Lifshitz that, in comparison to the zero-temperature case, the long-distance behavior of (12.23) is qualitatively different. For distances much greater than the thermal length scale introduced in Matsubara frequencies

$$z \gg \lambda_T \equiv \frac{\hbar c}{k_B T}, \qquad (12.26)$$

the atom-surface interaction energy behaves as:

$$\mathscr{V}(z) \stackrel{z\to\infty}{\sim} -\frac{k_B T\alpha_1(0)}{4(4\pi)\varepsilon_0 z^3}\frac{\varepsilon(0)-1}{\varepsilon(0)+1}. \qquad (12.27)$$

It is worth noting that the coefficient at the long distance $1/z^3$ asymptotics given by (12.27) vanishes for $T \to 0$, but the range of distances where it is valid, given by

(12.26), also widens. The distance scale of the temperature effects λ_T is usually orders of magnitude larger than the retardation distance scale $\bar{\lambda}$ and for experimentally considered cases the $1/z^4$ asymptotics given by (12.6) is valid for a wide range of distances. At room temperature λ_T is on the order of 100 µm (infrared wavelength), while λ is on the order of 100 nm for most ground state atoms (ultraviolet wavelength). For conductors, due to the singularity of $\varepsilon(\omega)$ at zero frequency, (12.27) takes a universal form independent of any characteristics of the solid. It remains a subject of current research whether or not this result requires modification. This peculiarity is especially pronounced for conductors with a very low concentration of carriers, or with slowly moving carriers (for example ions) [33].

12.3.6 Relativistic and Radiative Corrections

The theory of relativistic corrections to the interaction between closed shell atoms was recently developed by Pachucki [34]. Earlier studies of the interplay between relativistic and radiative corrections had been done by Meath and Hirschfelder [35, 36]. The general result is that the relativistic corrections of the lowest order (α^2) can be grouped into three categories, where the ones dominant at large interatomic distances (orbit-orbit, or Breit interaction) are already incorporated in the Casimir-Polder formula. Corrections can be classified as relativistic corrections to dynamic atomic polarizabilities, or as coupling between electric polarizability of one atom and the magnetic susceptibility of the other [34]. The relativistic and QED corrections to atomic polarizabilities are, at least for the well studied case of He, negligible at the level of precision considered here [37], and so are contributions from atomic magnetic susceptibility. On the other hand the contribution to the Casimir-Polder force resulting from the magnetic susceptibility of the solid can lead to measurable effects in the case of ferromagnetic materials [38].

12.3.7 Effects of Nonplanar Geometry and Nonuniformity

As described in the introductory chapter, many of the original experiments investigating the atom-surface interactions have been performed for geometries different from the planar one. The cases of an atom interacting with macroscopic spheres and cylinders (or wires) have been partly solved [39–41]. For more complicated geometries corrections can be estimated, at least for dielectric materials, using the pairwise summation method [5]. When the radius of curvature of the surface is much larger than the relevant range of atom-surface distances (which is frequently the case) the resulting geometric corrections are negligible. For all other cases, a first rigorous theoretical study on the inclusion of uniaxial corrugations has been performed for a scalar field by Gies et al. [42]. Unfortunately the extension of these results to electromagnetic fields is nontrivial. An important exception results from the fact that

even if the experiments are meant to be performed on flat surfaces, the nontrivial geometry enters in the form of corrections induced by corrugations or imperfections of the surface. In the limit of atom-surface distance much larger than the surface corrugations the roughness of the surface can be taken into account as a modification of its reflection coefficients [43].

The case when neither of the conditions mentioned above is fulfilled, which means that the curvature radius of the surface is neither very small nor very large in comparison to the atom-surface distance, and the surface is a conductor, is an open problem.

Modern Casimir-Polder Experiments

Modern experiments on atom-surface Casimir physics should not only be more sensitive and precise as a technique, but also be able to characterize and control the system under investigation in a quantitative manner. The first requirement is obvious; the second, however, no less important. Progress in this field will critically depend on the applicability of direct comparisons between theory and experiment and thus on the accuracy of the system parameters used on both sides. Let us relate this to the different type of modern Casimir-Polder experiments according to the approach they apply.

- Spectroscopic measurements: It is common knowledge in experimental physics that the best way for improving precision is to design a signature that can be measured as a frequency. In this respect the (quantum) optics experiments of the type mentioned above naturally promise a huge potential for Casimir-Polder physics. The atom-wall interaction leads to a distance-dependent shift of the atomic energy levels which may be detected by resonant spectroscopic techniques. An important and necessary requirement for this technique to work is that the energy shifts involved for the excited atoms behave very differently from those of the ground state species. The equilibrium between a repulsive light force and the attractive surface interaction can be used to establish a potential barrier. The barrier height can be controlled by changing the light field and its influence is then probed through the reflectivity for incident atoms [10]. For systems involving excited [44, 45] or Rydberg atoms [46, 47] additional resonance effects come into play, which may in fact turn the Casimir-Polder interaction itself into a repulsion (see for example [48]). Early experiments on the direct spectroscopic measurement of van der Waals forces have been successful up to a level of several tens of a percent [44, 46]. To date, it seems feasible to explore the progress in spectroscopic precision and to investigate the complex QED effects taking place during the atom-wall collisions an order of magnitude more accurately.
- Bose-Einstein condensates (BECs): From the manipulation of a BEC in front of a wall, information on the single atom-surface interaction can be obtained,

since all particles within this macroscopic quantum system are in the same
state. As the trap-minimum is moved closer towards the surface, the Casimir-
Polder forces change the curvature of the trapping potential which leads to a
relative change of the center of mass oscillation frequency. Cornell's group
measured this frequency shift for BEC atoms inside a chip-based trap [18, 49].
Refined measurements by the same group at the 10^{-4} level were interpreted by
Antezza et al. in terms of equilibrium and nonequilibrium thermal corrections
to the Casimir-Polder force [50]. The interaction strength was determined at a
ten percent level. In a recent proposal it was argued that the precision in this
type of BEC experiments may be improved by an order of magnitude through
the use of atomic clocks [51].

In both types of quantum optics experiments above it remains unclear how the
state of the surface and its deposits can be quantitatively measured and included
in theory. The same argument also holds for the deflection experiments by
Hinds et al. that rely on the fact that atoms are removed from the beam through
sticking. Absorbed atoms contaminate the substrate and modify the interaction
potential at a level that need not be constant, but may vary with the experi-
mental conditions, like time, light intensity and temperature. Even at sub-
monolayer coverage, adsorbates (in particular metallic ones) modify the
dielectric properties of the system. This is in fact one of the reasons why IR
spectroscopy is such a sensitive and well established tool in surface science (see
for example [52]). Benedek et al. [53] recently reviewed spectral consequences
of vibrations of alkali metal overlayers on metal surfaces, that depend very
sensitively on atomic mass, adsorption position, coverage and substrate ori-
entation. Pucci et al. [54] have recently found a strong enhancement of
vibration signals by coupling an antenna to surface phonon polaritons, using
(far) IR surface spectroscopy. In particular the investigation of temperature
effects in the Casimir-Polder physics may be strongly influenced by such
spectral features. Inversely, one could include (far) IR spectroscopy as a tool to
quantify the state of the substrate in future BEC experiments.

- Atom interference: Another very useful step for improving experimental pre-
cision is shifting from intensity measurements to phase sensitive quantities. The
experiments mentioned in Sect. 2 by Aspect [55] and Cronin [16] are examples
along this line. At the heart of both techniques is an atom interferometer, which
measures phase shifts in the de Broglie waves of the atoms. These first
experiments to detect surface-induced phase shifts were not accurate enough to
test the power law of the potential. Recently, however, by using the Toulouse
interferometer significant improvement could be reported [56]. The interaction
strength between an atom and the silicon nitride nano-grating was now deter-
mined with a precision of 6%. Since the setup was not equipped with any
surface analytical tools, the authors used a trick to reduce the effect of surface
contamination discussed above. By taking ratios of interaction strength coef-
ficients obtained for different atoms, they compared the van der Waals systems
at a level of better than 3%. It must be realized, however, that taking the ratio

between two C_3 values is good only to first order approximation: different atomic species adsorb differently onto the same surface, with distinguished temperature behavior and spectral features. In comparing the two, the dielectric property changes of the wall need not be exactly the same. Still, this method is a definite improvement and could be useful for other techniques as well.

- Quantum reflection: In 2002 Shimizu et al. reported on a giant quantum reflection of neon atoms from a ridged silicon surface [57]. The enhancement of reflectivity with respect to that from flat silicon surfaces was initially explained as resulting from the reduced effective matter density in the outermost region of the structured sample. At comparable distances, the interaction potential would consequently be weaker for the latter and that would enhance the so called "Bad Land" condition for quantum reflectivity at a given value of z. Later it was established that the giant reflectivity was not so much a consequence of a modification in the Casimir-Polder potential, but rather due to the collision process itself.[7,8] The explanation was modified, interpreting the process of grazing incidence over the ridged surface in terms of a Fresnel diffraction [58]. This explanation, however, ignores the modification of the Casimir-Polder potential due to the periodic structure. This prompted us to experimentally investigate the underlying question of including geometric effects in this QED phenomenon more systematically. Extensive studies on the quantum reflectivity of ground state He atoms from nano-structured substrates of different shape and material were performed. The results have not been published yet, but have already initiated great activity in theory to develop a method for embedding these structures in the scattering formalism. In addition, our experiments show that the non-additivity of the Casimir-Polder potential leads to a strong azimuthal dependence of the measured reflectivity. The data allow for a phenomenological power law description of the interaction, which has a different exponent along different azimuthal directions.

12.4.1 The Heidelberg Approach

Thermal atom beam scattering was founded in the early 20th century by Stern and Estermann [59, 60] to verify the wave nature of matter. With the advent of high quality supersonic jets, the method of diffracting a beam of atoms from a crystalline surface developed in the 80's into a powerful tool in surface science.

---

[7] The need for a more sophisticated explanation was supported by independent observations in Ketterle's laboratory. In experiments at normal incidence dedicated to extremely low density materials quantum reflection was never observed.

[8] Recently, similar experiments were performed in Gerhard Meijer's group, scattering He atoms from a periodic micro-structure. It could not be substantiated that the process observed is in fact quantum reflection.
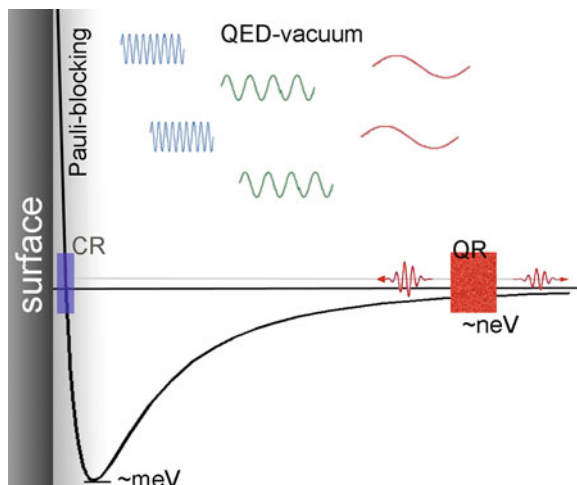
Fig. 12.3 Schematic representation of the full interaction potential between a neutral atom and the surface of a solid. At large distances, there is an attraction due to the Casimir-Polder and van der Waals effects. This region (marked QR) can be sampled by measuring the quantum reflectivity of an atomic beam impinging at grazing incidence. Close to the surface the interaction is dominated by an exponential repulsion, due to the Pauli blocking. The fraction of atoms scattering 'classically' from this wall can be used to extract in-situ information on the quality and the state of the surface on a sub-atomic level, like periodicity, corrugation, cleanliness and dynamics. Note that the typical energy ranges for these two processes differ by more than six orders of magnitude

"Classical" thermal atom scattering[9] is governed predominantly by the repulsive part of the full atom-surface interaction potential (see Fig. 12.3). This repulsion is due to Pauli exclusion during the partial overlap of the electron clouds of the atom and the solid at very short distances. The full interaction includes of course both the repulsive and attractive branches and shows a well of minimum potential energy.

The angular distribution of the specularly reflected atoms reveals information on the crystallinity and cleanliness of the exposed surface.[10] If the de Broglie wavelength of the atoms is on the order of the lattice constant of the crystal, Bragg diffraction may occur. The location of the diffraction peaks gives the periodicity of the surface structure, whereas their intensity distribution contains information on the corrugation height. With these signatures many detailed studies on clean and adsorbate covered substrates were performed. Within the impressive spectrum of

---

[9] The quotation marks merely indicate that scattering from a repulsive wall can of course be described according to the laws of classical physics. It should be clearly distinguished from quantum reflection, for which there is no classical analogue.

[10] Note that in the quantum mechanical formulation of atoms scattering from a repulsive wall, there always is a finite probability for the completely elastic channel.

achievements of this technique there are not only the crystallographic studies with sub-Angstrom resolution, but also a whole range of results on two dimensional dynamics, like surface phonon modes and charge density waves (to get a flavor of these accomplishments, see for example [61, 62] and references therein).

Thermal atom scattering is predominantly sensitive to potential features between the wall and the van der Waals range. Only limited information on the long distance Casimir-Polder contribution can be extracted from the scattering patterns. Physisorption and chemisorption processes, for example, are generally governed by the location and shape of the potential well near its energy minimum. The stronger bound states involved have their classical turning points generally near to the position of its minimum and normally also lie well within the non-retarded regime. They have been discussed to investigate quadrupolar and non-local effects in the physisorption of rare-gas atoms on metal surfaces [63].

Bound state resonance phenomena in atom-surface scattering [61, 62], however, are determined by the upper bound energy levels within the full interaction potential of 3. The outermost turning points of these higher levels are located at distances at which retardation effects may start playing a role. Analyzing all available data for helium, atomic and molecular hydrogen, however, Vidali et al. 64 established a surprising universality, indicating that these bound states lie still within the van der Waals regime. Choosing the mathematical shape of the repulsive wall to be exponential with distance $\sim \exp(-z/\sigma)$ and fixing the tail to be $\sim 1/z^3$ only, Vidali calculated the Bohr-Sommerfeld quantization condition for all bound state levels and plotted these with the experimental data (see Fig. 12.4). He found that independent of their type (metals, semiconductors and insulators) all measured systems fall onto the same curve. This impressive result suggests, that the adsorption potential energy functional form nearly universally takes the form of an exponential repulsion and a van der Waals attraction.

It remains worthwhile, however, to search for special cases in which the weakest bound state lies but barely underneath the dissociation limit. The outermost turning points may then be located at distances at which retardation effects are indeed important.[11] For such systems, bound state resonance experiments could indeed be a valuable tool in modern Casimir-Polder experimental physics, although maybe not a generic one.

About a decade ago, we designed a machine for performing atomic beam spin echo measurements on surfaces. Details on the experimental setup are given elsewhere [13]. In this apparatus, the nuclear magnetic moments of a flux of ^{3}He atoms are manipulated so as to obtain detailed information about (changes in) the velocity distribution of the beam before and after scattering from the surface. The ^{3}He beam is very slow (100 m/s $< v <$ 200 m/s), since the atomic beam source is cooled down to 1.1–4.2 K. The ^{3}He kinetic energy thus amounts to

---

[11] A famous example from atomic physics: the weak interaction between two neutral He atoms just happens to accommodate a single bound level at −150 neV only. As a consequence, the bond length in the He dimer is close to 45 Å!

Fig. 12.4 Plot from [64] illustrating the experimental correlation between energies of atom-surface bound states in units of potential well depth $|\varepsilon_n| = -E_n/D$ and $J(\varepsilon_n) = (n + \frac{1}{2})\hbar\pi/$ $(C_3^{1/3} D^{1/6}(2m)^{1/2})$ (reproduced with permission). The solid line is the prediction given by a simple model potential $V(z) = 3/(u-3)e^{-uz/a} - 1/(z+a)^3$ with constant u and a
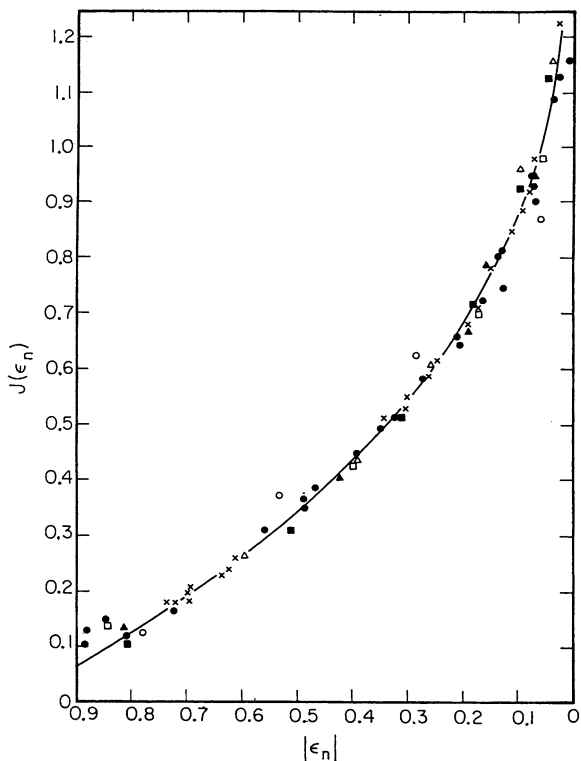
200–800 μeV, corresponding to a de Broglie wavelength λ_{dB} of 10–3 Å, or a wavevector $2\pi/\lambda_{dB}$ of 0.5–1.5 Å^{-1}. The He atoms are exclusively surface sensitive and have shown to probe corrugations at the surface down to some 0.01 Å [65]. The ^{3}He Atomic Beam Spin Echo method has been demonstrated to be a particularly sensitive and precise tool for characterizing the quality, structure and dynamics of clean, as well as adsorbate covered surfaces. As an example we summarize some of our results obtained with single crystal gold. In elastic ^{3}He diffraction experiments on the surface of single crystal Au(111), the dimensions of the reconstructed unit cell could be extracted to be $(p \times \sqrt{3})$, with $p = 21.5 \pm 0.5$ being expressed in the bulk gold nearest neighbor distance $a = 2.885$ Å. On top of this substrate, adsorbate molecules (coronene) were deposited and the structure at monolayer coverage was determined to be a commensurate (4×4) superstructure with respect to the unreconstructed gold surface. In addition, we studied diffusion of the diluted coronene molecules at submonolayer coverages. Their 2-D dynamics was shown to exhibit continuous and non-continuous (jump) 1-D diffusion. The activation barrier to this diffusion was inferred from an Arrhenius analysis of its temperature dependency. We investigated inelastic contributions to the scattering process and confirmed the existence and dispersion of anomalous phonon modes that are associated with the reconstruction.

Table 12.1 Problems limiting the accuracy of classical Casimir force measurements and corresponding solutions in the ^{3}He Atomic Beam Spin Echo technique

Casimir	versus	Casimir-Polder
Characterization of the surface quality		Surface science (typical <0.01 monolayer)
Quantization of surface roughness		Atom diffraction (single crystal)
Calibration of probe-surface distance		Atomic resolution
(plate-plate, sphere-plate)		(~ 0.01 Å)
Control over probe		Atomic beam
(sphere quality, coating, roughness)		($\sim 10^{19}$ He atoms s^{-1} sr^{-1})
Geometry		Atom size $\ll$ relevant length scale
(pl-pl: parallellism, sph-pl: proximity approx.)		(1 Å vs. 1 μm)
Spurious electrostatic effects		Neutral single atoms
Imperfect conductor		Any system (metal, semi-conductor, insulator)
Resolution		Atom interferometry

With the "classical" reflection governed by the repulsive and van der Waals regime of the potential, we have at our disposal an in-situ analytical tool from surface science. On the other hand, we can investigate He atoms being quantum reflected from the retarded regime and study Casimir-Polder physics. The advantages of such a powerful combination are summarized in the following Table 12.1.

In order to illustrate that this unique combination of tools is in fact at our disposal contemporaneously, we present here experimental data obtained for single crystal gold [66]. The measurements were performed much in the same way as our quantum reflection data described in Sect. 12.2 for the case of single crystal quartz were obtained [12]. The gold surface, however, is atomically flat[12] and also shows ^{3}He reflectivity from the repulsive wall (see Fig. 12.3).

Although both the "classical" and the quantum contributions consist of specularly reflected beams, the two can be distinguished through their line shape in the angular distribution. For each incident wave vector a detector angle scan was made and the two intensities evaluated. In this manner, the dots in upper set for the "classical" and the dots in lower set for the quantum reflectivities in Fig. 12.5 were obtained. The first curve in upper set is but a guide-to-the-eye for the classical reflection results. The first middle curve in lower set is an exact calculation based on the simple potential model used in 12.11, using the strength parameter for a perfect conductor. These quantum reflection data were also investigated with respect to the necessity for inhomogeneity of the model in 12.11. The additional curves in lower set in Fig. 12.5 clearly demonstrate that neither a strict van der Waals potential nor a pure Casimir-Polder attraction describe the data accurately. The dashed red line in lower set accounts for the homogeneous Casimir-Polder contribution (12.6), again using the interaction strength for a perfect conductor.

---

[12] In fact it is the exact same sample that was used in the surface science experiments reviewed earlier in this section.
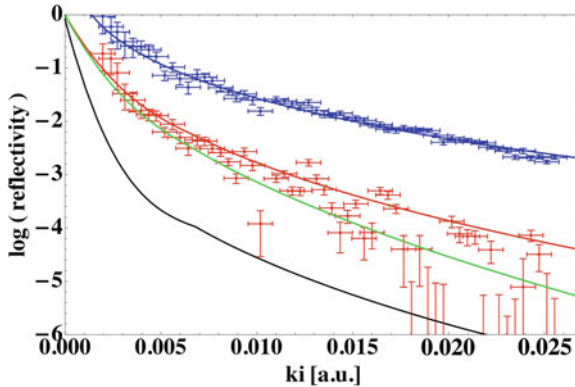
Fig. 12.5 Plot of the reflectivity of ^{3}He atoms from the single crystal surface of Au(111). The upper set of data points (including their statistical errors) represents "classical" reflection from the repulsive wall (see text). The lower set of data points and error bars corresponds to the simultaneously measured quantum reflectivity from the attractive tail of the interaction potential. Results for the corresponding simulation are shown in the lower three solid curves: the top one is based on the full potential derived from (12.19); the two lower curves are based on the homogeneous potentials for a perfect conductor, the Casimir-Polder result (12.6) (middle) and van der Waals result (12.5) (bottom), respectively. Finally, the bottom curve represents the homogeneous van der Waals result (12.5) for a perfect conductor. (Further details will be presented in [66].)

The corresponding homogeneous van der Waals interaction would give a quantum reflectivity, which is negligibly small. The second middle curve in lower set represents the quantum reflectivity based on a van der Waals interaction only, using the more realistic coefficient of $C_3 = 0.25$ eV Å^3. From the figure it is clear that at the distances explored in this experiment the energies are dominated by the Casimir-Polder interaction. Still, there is a definite need to include the van der Waals term explicitly. This demonstrates that with the Heidelberg approach it is now possible to resolve features in the potential at a few-percent level.

In summary, with the renaissance in atomic physics a great variety of new experimental techniques have been steadily improving the accuracy in Casimir-Polder measurements to well below the ten percent level. Current trends and proposals promise to be pushing this in the near future to below the one percent barrier. At that level of precision new contributions, like those explicitly dependent on temperature and higher order effects (additional multipoles, etc), are within reach. This will be important for our understanding of vacuum fluctuations. Tremendous theoretical progress has been made to include non-trivial boundary conditions to their spectrum. The feasibility of a direct comparison with measured data requires a quantitative experimental characterization of these conditions as well.

References

1. Casimir, H.B.G., Polder, D.: The influence of retardation on the London-van der waals forces. Phys. Rev. **73**(4), 360–372 (1948)
2. London, F.: Zur Theorie und Systematik der Molekularkräfte. Z. Phys. **63**(3–4), 245 (1930)
3. Verwey. E.J.W., Overbeek. J.T.G., van Nes. K.: (1947) J Phys. Colloid Chem. 51:631
4. Lifshitz. E., Pitaevskii. L.P.: (1956) Landau and Lifshitz course of theoretical physics: Statistical physics part 2. J. Exp.Theor. Phys. **2**:(73)
5. Parsegian, V.A.: Van der Waals Forces; A Handbook for Biologists, Chemists, Engineers, and Physicists. Cambridge University Press, New York (2006)
6. Sabisky, E.S., Anderson, C.H: Verification of the Lifshitz theory of the van der Waals potential using liquid-helium films. Phys. Rev. A **7**(2), 790–806 (1973)
7. Shih, A., Parsegian, V.A.: Van der Waals forces between heavy alkali atoms and gold surfaces: Comparison of measured and predicted values. Phys. Rev. A **12**(3), 835–841 (1975)
8. Dzyaloshinskii, I.E., Lifshitz, E.M., Pitaevskii, L.P: General theory of van der Waals forces. Adv. Phys. **29**, 165 (1961)
9. Sukenik, C.I., Boshier, M.G., Cho, D., Sandoghdar, V., Hinds, E.A.: Measurement of the Casimir-Polder force. Phys. Rev. Lett. **70**(5), 560–563 (1993)
10. Landragin, A., Courtois, J.Y., Labeyrie, G., Vansteenkiste, N., Westbrook, C.I., Aspect, A.: Measurement of the van der Waals force in an atomic mirror. Phys. Rev. Lett. **77**(8), 1464–1467 (1996)
11. Shimizu, F.: Specular reflection of very slow metastable neon atoms from a solid surface. Phys. Rev. Lett. **86**(6), 987–990 (2001)
12. Druzhinina, V., DeKieviet, M.: Experimental observation of quantum reflection far from threshold. Phys. Rev. Lett. **91**(19), 193,202 (2003)
13. DeKieviet, M., Dubbers, D., Schmidt, C., Scholz, D., Spinola, U.:^3He Spin echo: New atomic beam technique for probing phenomena in the neV range. Phys. Rev. Lett. **75**(10), 1919–1922 (1995)
14. Friedrich, H., Jacoby, G., Meister, C.G.: Quantum reflection by Casimir–van der Waals potential tails. Phys. Rev. A **65**(3), 032,902 (2002)
15. Friedrich, H., Trost, J.: Working with WKB waves far from the semiclassical limit. Phys. Rep. **397**(6), 359–449 (2004)
16. Perreault, J.D., Cronin, A.D.: Observation of atom wave phase shifts induced by van der Waals atom-surface interactions. Phys. Rev. Lett. **95**(13), 133,201–133,204 (2005)
17. Pasquini, T.A., Shin, Y., Sanner, C., Saba, M., Schirotzek, A., Pritchard, D.E., Ketterle, W.: Quantum reflection from a solid surface at normal incidence. Phys. Rev. Lett. **93**(22), 223,201–223,204 (2004)
18. McGuirk, J.M., Harber, D.M., Obrecht, J.M., Cornell, E.A.: Alkali-metal adsorbate polarization on conducting and insulating surfaces probed with Bose-Einstein condensates. Phys. Rev. A **69**(6), 062,905–062,910 (2004)
19. Lin, Y.J., Teper, I., Chin, C., Vuletić, V.: Impact of the Casimir-Polder potential and Johnson noise on Bose-Einstein condensate stability near surfaces. Phys. Rev. Lett. **92**(5), 050–404 (2004)
20. Obrecht, J.M., Wild, R.J., Antezza, M., Pitaevskii, L.P., Stringari, S., Cornell, E.A: Measurement of the temperature dependence of the Casimir-Polder force. Phys. Rev. Lett. **98**(6), 063,201–063,204 (2007)
21. Bender, H., Courteille, P.W., Marzok, C., Zimmermann, C., Slama, S.: Direct measurement of intermediate-range Casimir-Polder potentials. Phys. Rev. Lett. **104**(8), 083,201–083,204 (2010)
22. Saniz, R., Barbiellini, B., Platzman, P.M., Freeman, A.J.: Physisorption of positronium on quartz surfaces. Phys. Rev. Lett. **99**(9), 096,101–096,104 (2007)
23. Łach, G., DeKieviet, M., Jentschura, U.D: Multipole effects in atom-surface interactions: A theoretical study with an application to He–α-quartz. Phys. Rev. A **81**(5), 052–507 (2010)

24. Palik, E.D.: Handbook of Optical Constants of Solids. Academic Press, San Diego (1985)
25. Derevianko, A., Porsev, S.G., Babb, J.F.: Electric dipole polarizabilities at imaginary frequencies for the alkali-metal, alkaline-earth, and inert gas atoms. arXiv:0902.3929v1 p.16 (2009)
26. Marvin, A.M., Toigo, F.: Van der Waals interaction between a point particle and a metallic surface. II. Applications. Phys. Rev. A **25**(2), 803–815 (1982)
27. Milonni, P.W.: The Quantum Vacuum: An Introduction to Quantum Electrodynamics. Academic Press, San Diego (1994)
28. McLachlan, A.D.: Van der Waals forces between an atom and a surface. Mol. Phys. Int. J. Int. Chem. Phys. **7**, 381 (1964)
29. Hutson, J.M., Fowler, P., Zaremba E.: Quadrupolar contributions to the atom-surface Van der Waals interaction. Surf. Sci. **175**, 775–781 (1986)
30. Lach, G., DeKieviet, M.F.M., Jentschura, U.D.: Noble gas, alkali and alkaline atoms interacting with a gold surface. Int. J. Mod. Phys. A **25**(11),2337–2344 (2010)
31. Babb, J.F., Klimchitskaya, G.L., Mostepanenko, V.M.: Casimir-Polder interaction between an atom and a cavity wall under the influence of real conditions. Phys. Rev. A **70**(4), 042,901–042,912 (2004)
32. Mostepanenko, V.M., Trutnov, N.N.: The Casimir Effect and Its Applications. Clarendon Press, Oxford (1997)
33. Pitaevskii, L.P.: Thermal Lifshitz force between an atom and a conductor with a small density of carriers. Phys. Rev. Lett. **101**(16), 163–202 (2008)
34. Pachucki, K.: Relativistic corrections to the long-range interaction between closed-shell atoms. Phys. Rev. A **72**(6), 062–706 (2005)
35. Meath, W.J., Hirschfelder, J.O.: Long-range (retarded) intermolecular forces. J. Chem. Phys. **44**(9), 3210–3215 (1966)
36. Meath, W.J., Hirschfelder, J.O: Relativistic intermolecular forces, moderately long range. J. Chem. Phys. **44**(9), 3197–3209 (1966)
37. Łach, G., Jeziorski, B., Szalewicz, K.: Radiative corrections to the polarizability of helium. Phys. Rev. Lett. **92**(23), 233001 (2004)
38. Bimonte, G., Klimchitskaya, G.L., Mostepanenko, V.M.: Impact of magnetic properties on atom-wall interactions. Phys. Rev. A **79**(4), 042,906–043,912 (2009)
39. Marvin, A.M., Toigo, F.: Van der Waals interaction between a point particle and a metallic surface. I. Theory. Phys. Rev. A **25**(2), 782–802 (1982)
40. Buhmann, S.Y., Dung, H.T., Welsch, D.G.: The van der Waals energy of atomic systems near absorbing and dispersing bodies. J. Opt. B: Quantum and Semiclassical Opt. **6**(3), S127 (2004)
41. Klimchitskaya, G.L., Blagov, E.V., Mostepanenko, V.M.: Casimir-Polder interaction between an atom and a cylinder with application to nanosystems. J. Phys. A Math. Gen. **39**(21), 6481 (2006)
42. Döbrich B., DeKieviet, M., Gies, H.: Scalar Casimir-Polder forces for uniaxial corrugations. Phys. Rev. D **78**(12), 25022 (2008)
43. Celli, V., Marvin, A., Toigo, F.: Light scattering from rough surfaces. Phys. Rev. B **11**(4), 1779–1786 (1975)
44. Failache, H., Saltiel, S., Fichet, M., Bloch, D., Ducloy, M.: Resonant van der Waals repulsion between excited Cs atoms and sapphire surface. Phys. Rev. Lett. **83**(26), 5467–5470 (1999)
45. Gorza, M.P., Saltiel, S., Failache, H., Ducloy, M.: Quantum theory of van der Waals interactions between excited atoms and birefringent dielectric surfaces. Eur. Phys. J. D **15**, 113–126 (2001)
46. Sandoghdar, V., Sukenik, C.I., Hinds, E.A., Haroche, S.: Direct measurement of the van der Waals interaction between an atom and its images in a micron-sized cavity. Phys. Rev. Lett. **68**(23), 3432–3435 (1992)
47. Anderson, A., Haroche, S., Hinds, E.A., Jhe, W., Meschede, D.: Measuring the van der Waals forces between a Rydberg atom and a metallic surface. Phys. Rev. A **37**(9), 3594–3597 (1988)

48. Failache, H., Saltiel, S., Fichet, M., Bloch, D., Ducloy, M.: Resonant coupling in the van der Waals interaction between an excited alkali atom and a dielectric surface: An experimental study via stepwise selective reflection spectroscopy. Eur. Phys. J. D **23**, 237 (2003)
49. Harber, D.M., Obrecht, J.M., McGuirk, J.M., Cornell, E.A.: Measurement of the Casimir-Polder force through center-of-mass oscillations of a Bose-Einstein condensate. Phys. Rev. A **72**(3), 033,610–033,615 (2005)
50. Obrecht, J.M., Wild, R.J., Antezza, M., Pitaevskii, L.P., Stringari, S., Cornell, E.A.: Measurement of the temperature dependence of the Casimir-Polder force. Phys. Rev. Lett. **98**(6), 063,201–063,204 (2007)
51. Derevianko, A., Obreshkov, B., Dzuba, V.A.: Mapping out atom-wall interaction with atomic clocks. Phys. Rev. Lett. **103**(13), 133,201–133,204 (2009)
52. Trenary, M.: Reflection absorption infared spectroscopy and the structure of molecular adsorbates on metal surfaces. Annu. Rev. Phys. Chem. **51**(1), 381–403 (2000)
53. Rusina, G.G., Eremeev, S.V., Echenique, P.M., Benedek, G., Borisova, S.D., Chulkov, E.V.: Vibrations of alkali metal overlayers on metal surfaces. J. Phys. Condens. Matter **20**(22), 224007 (2008)
54. Neubrech, F., Weber, D., Enders, D., Nagao, T., Pucci, A.: Antenna sensing of surface phonon polaritons. J. Phys. Chem. **114**, 7299 (2010)
55. Marani, R., Cognet, L., Savalli, V., Westbrook, N., Westbrook, C.I, Aspect, A.: Using atomic interference to probe atom-surface interactions. Phys. Rev. A **61**(5), 053–402 (2000)
56. Lepoutre, S., Jelassi, H., Lonij, V.P.A., Trenec, G., Buchner, M., Cronin, A.D., Vigue, J.: Observation of atom wave phase shifts induced by van der Waals atom-surface interactions. EPL **88**, 200002 (2009)
57. Shimizu, F., Fujita, J.I.: Giant quantum reflection of neon atoms from a ridged silicon surface. J. Phys. Soc. Jpn. **71**(1), 5–8 (2002)
58. Oberst, H., Kouznetsov, D., Shimizu, K., Fujita, J.I., Shimizu, F.: Fresnel diffraction mirror for an atomic wave. Phys. Rev. Lett. **94**(1), 013–203 (2005)
59. Stern, O.: Beugung von molekularstrahlen am gitter einer krystallspaltflche. Naturwissenschaften **17**, 391 (1929)
60. Estermann, L., Stern, O.: Beugung von molekularstrahlen. Z. Phys. **61**, 95 (1930)
61. Benedek, G., Valbusa U.: Dynamics of Gas-Surface Interaction.Vol. 21. Springer Series in Chemical Physics, Berlin (1982)
62. Scoles, G.: Atomic and Molecular Beam Methods. Oxford University Press, New York, vol. I and II. (1988)
63. Girard, C., Humbert, J.: Quadrupolar and non-local effects in the physisorption of rare-gas atoms on metal surfaces. Chem. Phys. **97**, 87–94 (1985)
64. Vidali, G., Cole, M.W., Klein, J.R.: Shape of physical adsorption potentials. Phys. Rev. B **28**(6), 3064–3073 (1983)
65. DeKieviet, M., Dubbers, D., Klein, M., Pieles, U., Skrzipczyk, M.: Surface science using molecular beam spin echo. Surf. Sci. **377**(379), 1112–1117 (1997)
66. Stöferle, T., Warring, U., Lach, G., Jentschura, U.D., DeKieviet, M.F.M.: Quantum and classical reflection of He from single crystal gold. Manuscript in preparation (2011)